Superconductivity and Electron Tunneling

Abstract: Experiments on the tunneling of electrons through a thin dielectric layer separating two superconducting metals are reported. Data are presented for the pairs Al-Pb, Sn-Pb, and In-Sn. Particular attention is paid to the form of the tunneling current vs voltage characteristics and to the changes observed as a function of temperature. Experimental details relative to the measurement techniques, the preparation of the samples, and the preparation of the dielectric layers are presented. An analysis of the problem is presented which is based on the simple, one-dimensional model of the electron energy spectrum of a superconductor given by the theory of Bardeen, Cooper, and Schrieffer. Close quantitative agreement is obtained between the results of the calculations and the observed characteristics.

Introduction

Much attention has recently been devoted to the problem of electron tunneling through thin dielectric layers between two metals, 1-3 one or both of which were superconducting. Observation at small voltages revealed a linear tunneling current vs voltage characteristic when both metals were normal, the appearance of a nonlinear region when one metal became superconducting and, further, the appearance of a negative resistance region when both metals were superconducting. The measurements were interpreted in terms of a simple, one-dimensional model of the electron energy spectrum of a superconductor, namely that given by the theory of Bardeen, Cooper, and Schrieffer (BCS).4 It was shown that the experiments provided a direct measure of the energy gap of a superconductor. Certain assumptions were necessary, the most stringent being that the probability for electron transfer through the barrier can be treated as constant over the range of energies of interest. Recently Bardeen⁵ has found it plausible to take the tunneling probability as constant when interpreting such experiments.

In their Letter, Nicol, Shapiro, and Smith² presented the essentials of the analysis and a comparison with experiment of certain preliminary results of machine computation based upon that analysis.⁶ This paper gives complete details of the analysis, in particular as

they relate to the reduction of the expressions involved to a form suitable for machine computation. The calculations are carried through entirely within the spirit of the simple model provided by the BCS theory, together with the simplifying assumption referred to above. In particular, the density-of-states curve given by BCS is used unmodified by any rounding-off parameter.⁷ The predictions of the analysis are compared with the results of experiments on the superconducting pairs Al-Pb, Pb-Sn, and Sn-In. Comparison of the measured temperature dependence of the energy gap for Sn with that predicted by BCS is also included.

The calculations reveal the existence of a symmetric, logarithmic singularity in the current at the lower voltage limit of the negative resistance region and a finite, discontinuous current jump at the upper voltage limit. The effect of the finite lifetime of the excited states of a superconductor is to remove the singularity, although a cusp-like peak remains, and to spread the current jump over a small voltage interval. When allowance is made for this effect, close quantitative agreement is obtained with experiment.

Some applications of the tunneling technique to other problems in superconductivity are mentioned.

Analysis

Figure 1 is a sketch of the electron energy spectrum in a small energy interval about the Fermi level for a sandwich formed of two different superconductors

Advanced Research Division, Arthur D. Little, Inc.

[†] Engineering Division, Arthur D. Little, Inc.

separated by a thin dielectric layer. In the absence of an applied voltage, the Fermi levels for both metals lie at the same energy. When a voltage is applied, the energy spectrum for one metal shifts with respect to that of the other metal by the energy equivalent of the voltage. The convention adopted in Fig. 1 will be used throughout the paper; namely, positive voltage is applied to Metal 1, and Metal 2 is considered shifted in energy with respect to Metal 1.

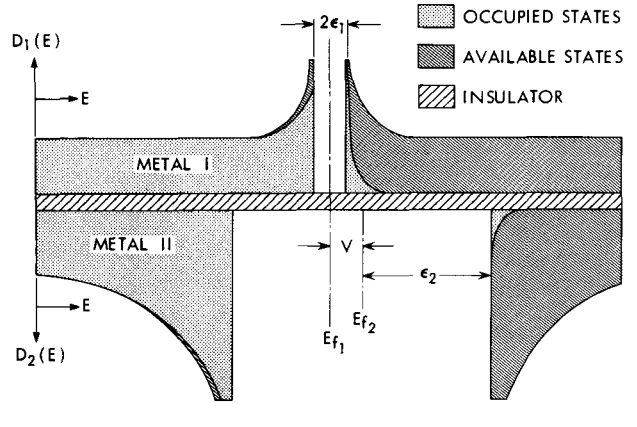
For the simple one-dimensional model, the one-way tunneling current is proportional to an integral over all energies of the product of the number of electrons in one metal by the number of unoccupied states (holes) in the other metal at the corresponding energy times the probability for an electron at that energy to tunnel through the barrier. The net current is given by the difference in the opposed one-way currents. It is convenient to take the energy zero at the Fermi level for Metal 1, E_{f1} , and to express all energies in units of kT. Then

$$I\alpha \int_{-\infty}^{\infty} \{\rho_{2}(E-V)f(E-V)\rho_{1}(E)[1-f(E)]P_{2\to 1} -\rho_{2}(E-V)[1-f(E-V)]\rho_{1}(E)f(E)P_{1\to 2}\} dE, \quad (1)$$

where V is the energy equivalent of the applied voltage, ρ_1 and ρ_2 are the density-of-states functions for Metals 1 and 2 respectively, $P_{2\rightarrow 1}$ and $P_{1\rightarrow 2}$ are the probabilities of an electron tunneling from Metal 2 to Metal 1, and vice-versa, and f(E) is the Fermi function,

$$f(E) = 1/(1 + e^{E})$$
. (2)

Figure 1 The density-of-states function and the filled states sketched in a small energy interval about the Fermi level for a sandwich formed of two different superconductors separated by a thin insulating layer. A positive voltage, V, is applied to Metal 1.



D (E) = DENSITY OF STATES

For mathematical convenience, the lower limit of integration is extended to $-\infty$, although strictly it should be taken as $-E_{f1}$. Because of the action of the Fermi functions, the important region of integration is confined to an interval of a few kT about the Fermi level. With the assumption that the tunneling probability is constant over this energy interval and that $P_{2\rightarrow 1}$ is equal to $P_{1\rightarrow 2}$, Eq. (1) reduces to

I = const

$$\times \int_{-\infty}^{\infty} \rho_2(E-V)\rho_1(E)[f(E-V)-f(E)] dE, (3)$$

which is Eq. (3) of Ref. 2.

If $\rho_n(E)$ is the density-of-states in the normal state, then $\rho_s(E)$, the density-of-states in the superconducting state, ⁴ differs from it by a factor $G(E, \varepsilon)$,

$$\rho_{s}(E) = G(E, \varepsilon)\rho_{n}(E) \tag{4}$$

with

$$G(E,\varepsilon) = \left| E \middle| RP \left\{ \frac{1}{\left[E^2 - \varepsilon(T)^2 \right]^{\frac{1}{2}}} \right\}, \tag{5}$$

where $2\varepsilon(T)$ is the temperature-dependent energy gap and RP designates the real part. $\rho_n(E)$ is, generally, only slowly varying in the vicinity of the Fermi level, especially in comparison with $G(E, \varepsilon)$. In the following, $\rho_n(E)$ shall be taken as constant for both Metals 1 and 2 at the value it has at the Fermi level. In Eq. (3) it is convenient to combine these two constants into the proportionality constant and to use a system of current units such that the proportionality constant has the value unity.

Three cases are of interest.

Case I. Both metals normal. The current is given by

$$I = \int_{-\infty}^{\infty} \phi(E, V) dE, \qquad (6)$$

where

$$\phi(E, V) = \left[\frac{1}{1 + \exp(E - V)} - \frac{1}{1 + \exp E} \right]$$

$$= \frac{\exp E[1 - \exp(-V)]}{[1 + \exp(E - V)][1 + \exp E]}.$$
 (7)

This case has been discussed by Giaever¹ and by Fisher and Giaever⁹ and will not be further examined here except to note that the observed features of the I-V characteristic, namely symmetry in the origin and I proportional to V, are easily obtained from Eqs. (6) and (7), provided V is small relative to the Fermi energy.

Case II. One metal superconducting. The current is given by

$$I = \int_{-\infty}^{\infty} G(E - V, \varepsilon) \phi(E, V) dE.$$
 (8)

Since $G(E - V, \varepsilon)$ is discontinuous at $E = V \pm \varepsilon$, the range of integration must be subdivided at those points. Let

$$I = I_1 + I_2$$

$$I_1 = -\int_{-\infty}^{V-\varepsilon} \frac{(E-V)}{\sqrt{(E-V)^2 - \varepsilon^2}}$$

$$\times \left\{ \frac{1}{1 + \exp(E-V)} - \frac{1}{1 + \exp E} \right\} dE \qquad (9)$$

$$I_2 = \int_{V+\varepsilon}^{\infty} \frac{(E-V)}{\sqrt{(E-V)^2 - \varepsilon^2}}$$

$$\times \left\{ \frac{1}{1 + \exp(E-V)} - \frac{1}{1 + \exp E} \right\} dE .$$

In both of these integrals let

$$u = [(E - V)^2 - \varepsilon^2]^{\frac{1}{2}}.$$
 (10)

Note that in I_1 this is interpreted to mean

$$E = V - \left[u^2 + \varepsilon^2\right]^{1/2}, \tag{11}$$

while in I_2 ,

$$E = V + \left[u^2 + \varepsilon^2 \right]^{\frac{1}{2}}. \tag{12}$$

As a result of this substitution the singularities are removed from the real axis and the following relations are obtained:

$$\begin{cases} I_1 = \int_0^\infty \frac{\exp V - 1}{(1 + \exp r)(1 + \exp[V - r])} du \\ I_2 = \int_0^\infty \frac{\exp V - 1}{(1 + \exp[-r])(1 + \exp[V + r])} du \end{cases}, \tag{13}$$

where $r = [u^2 + \varepsilon^2]^{\frac{1}{2}}$.

These integrals can be evaluated numerically on a reasonably coarse mesh. Since, for large values of u, the integrand decays exponentially with u, a simple rule for terminating the integration can be found by writing the asymptotic expansion of

$$A = \int_{a}^{\infty} \exp(-\sqrt{u^{2} + \varepsilon^{2}}) du$$

$$\sim \frac{\sqrt{a^{2} + \varepsilon^{2}}}{a} \exp(-\sqrt{a^{2} + \varepsilon^{2}}) + \cdots$$
(14)

Obviously, therefore, as soon as the integrand becomes negligible the remainder of the integral is also negligible.

Computations based on integrals (13) have been reported and discussed as Fig. 2 of Ref. 2. Excellent quantitative agreement is obtained with the results of experiments employing Pb in the superconducting state and Al in the normal state.

Case III. Both metals superconducting. The current is given by

$$I = \int_{-\infty}^{\infty} G(E, \, \varepsilon_1) G(E - V, \, \varepsilon_2)$$

$$\times \left[\frac{1}{1 + \exp(E - V)} - \frac{1}{1 + \exp E} \right] dE . \tag{15}$$

Singular points may occur at $E=\pm \varepsilon_1$, $V\pm \varepsilon_2$. Some of the singular points may be suppressed for certain ranges of the voltage, and at particular values of V certain of them may coincide. Without loss of generality it may be assumed that $\varepsilon_1 \leq \varepsilon_2$ and V>0 (for V=0, obviously I=0).

It is now clear that three ranges of V must be investigated. In fact,

$$\begin{split} I &= I_1 + I_2 \;, & 0 < V < \varepsilon_2 - \varepsilon_1 \\ I &= I_2 + I_3 \;, & \varepsilon_2 - \varepsilon_1 < V < \varepsilon_2 + \varepsilon_1 \\ I &= I_2 + I_3 + I_4 \;, \; \varepsilon_2 + \varepsilon_1 < V, \end{split}$$

where

$$I_{1} = -\int_{-\infty}^{V-\varepsilon_{2}} \frac{E(V-E)}{\sqrt{E^{2}-\varepsilon_{1}^{2}}\sqrt{(V-E)^{2}-\varepsilon_{2}^{2}}} \times \phi(E, V) dE$$

$$I_{2} = \int_{V+\varepsilon_{2}}^{\infty} \frac{E(E-V)}{\sqrt{E^{2}-\varepsilon_{1}^{2}}\sqrt{(E-V)^{2}-\varepsilon_{2}^{2}}} \times \phi(E, V) dE$$

$$I_{3} = -\int_{-\infty}^{-\varepsilon_{1}} \frac{E(V-E)}{\sqrt{E^{2}-\varepsilon_{1}^{2}}\sqrt{(V-E)^{2}-\varepsilon_{2}^{2}}} \times \phi(E, V) dE$$

$$I_{4} = \int_{\varepsilon_{1}}^{V-\varepsilon_{2}} \frac{E(V-E)}{\sqrt{E^{2}-\varepsilon_{1}^{2}}\sqrt{(V-E)^{2}-\varepsilon_{2}^{2}}} \times \phi(E, V) dE$$

$$\times \phi(E, V) dE$$

$$\times \phi(E, V) dE$$

with $\phi(E, V)$ given by Eq. (7).

In I_1 and I_3 the sign of E is changed to yield

$$\begin{cases}
I_{1} = \int_{\varepsilon_{2}-V}^{\infty} \frac{E(E+V)}{\sqrt{E^{2}-\varepsilon_{1}^{2}}\sqrt{(E+V)^{2}-\varepsilon_{2}^{2}}} \\
\times \phi(-E,V) dE \\
I_{3} = \int_{\varepsilon_{1}}^{\infty} \frac{E(E+V)}{\sqrt{E^{2}-\varepsilon_{1}^{2}}\sqrt{(E+V)^{2}-\varepsilon_{2}^{2}}} \\
\times \phi(-E,V) dE .
\end{cases}$$
(17)

The integrands of I_1 , I_2 , and I_3 are singular at the lower limit of integration, while the integrand of I_4 is singular at both limits. The technique for disposing of these singularities, in order to permit numerical

integration, is essentially the same in all cases and will be illustrated by a consideration of I_1 .

The denominator of the integrand of I_1 may be written as

$$D = \sqrt{(E - \varepsilon_1)(E + V - \varepsilon_2)} \times \sqrt{(E + \varepsilon_1)(E + V + \varepsilon_2)}.$$
(18)

The singular behavior of the integrand stems from the first square root only; the rest of the integrand is tractable. In order to deal with this singularity let

$$E = \alpha \cosh u + \beta \,, \tag{19}$$

and let α and β be determined so that

$$(E - \varepsilon_1)(E + V - \varepsilon_2) \equiv \alpha^2 \sinh^2 u . \tag{20}$$

In this case

$$\begin{cases} \alpha = \frac{1}{2}(\varepsilon_2 - \varepsilon_1 - V) \\ \beta = \frac{1}{2}(\varepsilon_2 + \varepsilon_1 - V) . \end{cases}$$
 (21)

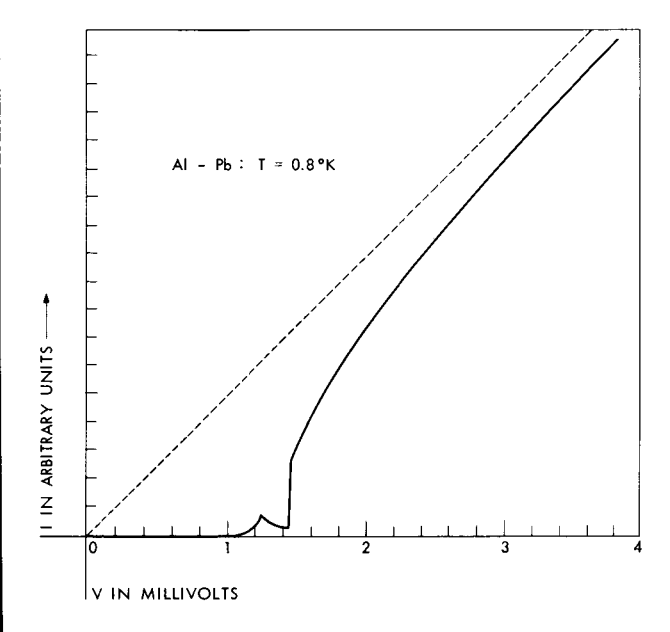
Now

$$dE = \alpha \sinh u \, du \,, \tag{22}$$

so that the factor $\sinh u$ in the denominator of the integrand cancels when the substitution for E is made. Finally, therefore,

$$I_{1} = \int_{0}^{\infty} \frac{E(E+V)}{\sqrt{(E+\varepsilon_{1})(E+V+\varepsilon_{2})}} \, \phi(-E, V) \, du \,, \quad (23)$$

Figure 2 Voltage vs tunneling current characteristic (solid line) calculated for an Al-Pb sandwich at 0.8°K. The current is normalized so that the normal state resistance is represented by a line (dashed) with a 45° slope. Experimental values for the energy gaps were used in the calculations.



where

$$E = \frac{1}{2}(\varepsilon_2 - \varepsilon_1 - V)\cosh u + \frac{1}{2}(\varepsilon_2 + \varepsilon_1 - V). \tag{24}$$

The integrals I_2 and I_3 also yield to similar substitutions of the form of Eq. (19), and since for large values of u the integrands behave as $\exp(-\cosh u)$, the numerical integration process can be safely terminated as soon as the integrand is negligible.

The integral I_4 is also quite similar, but requires the substitution of a circular rather than a hyperbolic function. The result is that

$$I_{4} = \int_{-\pi/2}^{\pi/2} \frac{E(V - E)}{\sqrt{(E + \varepsilon_{1})(V - E + \varepsilon_{2})}} \, \phi(E, V) \, du \,\,, \quad (25)$$

where

$$E = \frac{1}{2}(V - \varepsilon_1 - \varepsilon_2)\sin u + \frac{1}{2}(V + \varepsilon_1 - \varepsilon_2). \tag{26}$$

Note that in I_1 the value of E is constant when $V=\varepsilon_2-\varepsilon_1$. Since the range of integration is unlimited, the value of I_1 will be infinite. The mathematical singularity in the current is of a logarithmic type (cf. Appendix). This result is a consequence of using the strict BCS form of the density-of-states, a function which itself has a singularity. For a real system the density-of-states would be rounded-off. For such a modified function the infinity in current would be removed. The analysis does predict a sharp, symmetric, cusp-like peak of current within a narrow range of voltage about $V=\varepsilon_2+\varepsilon_1$ because of the logarithmic nature of the mathematical singularity.

The integrand of I_4 is likewise a constant when $V = \varepsilon_1 + \varepsilon_2$. Since the range of integration is finite, I_4 can be readily evaluated at this voltage. The result is

$$I_{4}^{*} = \pi/2\sqrt{\varepsilon_{1}\varepsilon_{2}} \times \left\{ \frac{1 - \exp(-\varepsilon_{1} - \varepsilon_{2})}{[1 + \exp(-\varepsilon_{1})][1 + \exp(-\varepsilon_{2})]} \right\}.$$
 (27)

Thus the analysis predicts a discontinuity in the graph of the current when $V = \varepsilon_1 + \varepsilon_2$, and also predicts that the height of the current jump will be proportional to I_4^* . A typical calculated curve for a Pb-Al sandwich is shown in Fig. 2. Experimental values for the energy gaps were used in the calculations. Again, for a real system, one consequence of the rounding-off of the density-of-states curve would be to spread the current jump over a small region of voltage about the value $V = \varepsilon_1 + \varepsilon_2$.

Experimental details

Most experiments involved vacuum-deposited metal films. Samples were prepared by depositing a strip of metal on a glass substrate, overlaying the strip with a thin dielectric layer formed in a variety of ways, and then depositing up to three cross strips of another metal. Figure 3 shows such a sample ready for testing. For the Al-Pb sandwiches, the Al was deposited first

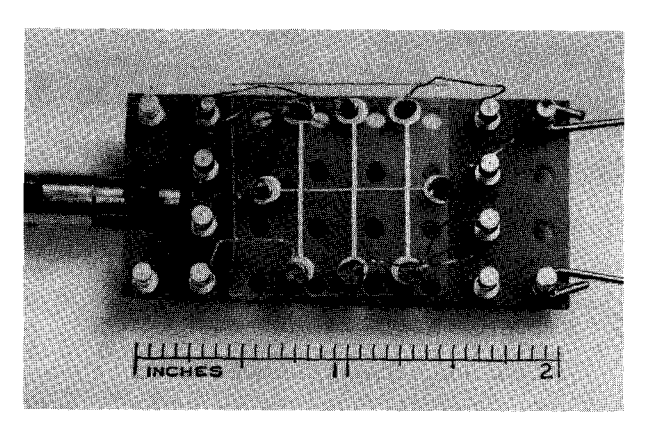
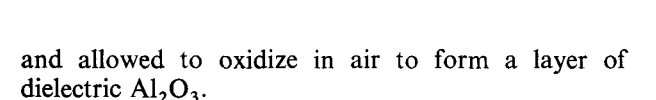


Figure 3 Typical specimen, showing three tunneling sandwiches.



For other samples, monolayers of barium stearate were used as the dielectric barrier. 10 The technique for forming and transferring such monolayers has been known for some time and is described by Blodgett and Langmuir. 11 Briefly, the procedure is to spread stearic acid dissolved in benzene on the surface of a dilute aqueous solution of barium carbonate. The acid spreads with its carboxyl group in contact with the water and its hydrocarbon chain nearly vertical. The molecules can then be compressed into a closely packed monolayer by use of a piston oil. The extent of conversion of the monolayer to barium stearate is controlled by the pH of the solution. Films are transferred to a solid surface by passing the glass substrate, with a metal strip already deposited on it, through the surface of the aqueous solution.

For most measurements an alternating current at some audio frequency was passed from one metal strip to the other and the voltage across the dielectric layer displayed on an oscilloscope as a function of the current. Conditions approximated constant voltage operation. A specially built curve tracer incorporating a number of convenient features was employed. The resistance of each metal film was also measured. The upper frequency of operation was limited to about 400 cps by relative phase shift in the amplifiers. The shape of the *V-I* traces obtained was independent of the observation frequency.

The sample was immersed in liquid helium at 4.2°K and below. Temperatures as low as 0.8°K were obtained by pumping on the liquid helium bath. Temperature was determined from the liquid helium vapor pressure or from a carbon resistance thermometer. By appropriate choice of temperature, the tunneling characteristics could be obtained for both metals normal or one or both metals superconducting.

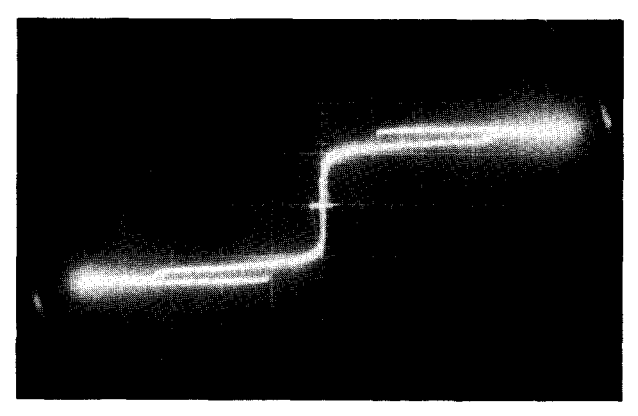


Figure 4 Double-exposure photograph of the V-I characteristic of an Al-Pb sandwich at 1.28°K (smaller negative resistance region) and at 1.00°K. The voltage scale (vertical) is 1 mv per large division, and the current scale is 10 µamp per large division.

Experimental results

The analysis of the second Section bears out the contention² that the voltage vs tunneling current characteristic measured for a sandwich formed of two superconducting metals separated by a thin dielectric layer provides a direct measure of the energy gap of a superconductor. That the qualitative features of the analysis are in agreement with experiment is readily apparent from Figs. 4, 5, and 6.

Figure 4 is a double-exposure photograph of the V-I characteristic of an Al-Pb sandwich at two different temperatures. In one trace, taken at 1.28°K, a temperature just below that at which the Al became superconducting, the negative resistance region is just noticeable, corresponding to the very small energy gap in Al near its transition temperature. In the other trace, taken at 1.00°K, the negative resistance region is much more extensive, corresponding to the extent of the energy gap in Al at a temperature substantially below the transition temperature. On the other hand, the value of voltage at which the midpoint of the negative resistance region occurs has remained unaffected by the change in temperature. This corresponds to the energy gap in the Pb having attained its full limiting value, since both temperatures are well below the Pb transition temperature of 7.2°K. To facilitate comparison, reference may be made to Fig. 8, which contains a plot of the variation of energy gap with reduced temperature as predicted by BCS.

In Fig. 5, V-I characteristics taken at three different temperatures for a Sn-Pb sandwich are reproduced in a manner making intercomparison particularly simple. From bottom to top, the three characteristics are for temperatures of 3.75°K, 3.70°K, and 3.60°K, respectively. Note particularly the gradual opening up in voltage of the extent of the negative resistance region corresponding to the increase in the magnitude of the

energy gap in Sn with decreasing temperature. The gap in Pb at these temperatures is practically at its full limiting value. Thus, from Eq. (27), the magnitude of the current jump which occurs just at the high voltage end of the negative resistance region should also increase as the temperature decreases, since the jump is approximately proportional to the square root of the Sn gap. That this does occur is very clear from the figure.

Figure 6 shows, with an expanded current scale, a portion of a *V-I* characteristic for a Sn-Pb sandwich. The cusp-like peak in the current at the lower voltage end of the negative resistance region is evident as predicted by the Analysis Section. The break in the characteristic within the negative resistance region is attributed to the onset of oscillation.

Figures 7a, 7b, and 7c give a quantitative comparison between the analysis and experiment for a Sn-Pb sandwich at 3.40°K, 3.60°K, and 3.70°K, respectively. The experimental points were determined from photographs such as that shown in Fig. 5. The current at each temperature was normalized so that the points marked by arrows fell on the calculated curve. The crossing area through which tunneling occurred (cf. Fig. 3) was approximately 0.1 mm². In the calculations the experimental values of the energy gaps were used. The agreement between the calculated curve and the experimental points is excellent except

that the current jump is spread over a small region of voltage and is not discontinuous. Figure 8 shows a comparison with the experimentally determined temperature dependence of the energy gap for superconducting tin and that predicted by the BCS theory. Again the agreement is excellent.

The limiting full values of the energy gaps for superconducting Al, Pb, and Sn, as determined from experiments involving tunneling between superconductors, are given in Table 1.

Data were also taken for Sn-In sandwiches. Here swept dc was applied to the sample and, after suitable amplification, the V-I characteristic was plotted on an X-Y recorder. Figure 9 shows a typical characteristic taken at 1.98°K. It is immediately apparent that no negative resistance region is present. Furthermore, what has earlier been characterized as the current jump is, in Fig. 9, spread over an appreciable region of voltage. Although the energy gaps for Sn and In are not immediately obtainable from Fig. 9, they are expected to be nearly equal. Calculations were carried out using the formulas of the Analysis Section, in which the previously determined value of the gap for Sn was used together with an average value for the In gap obtained from the literature. 13 It is clear from these calculations (cf., for example, Figs. 10 and 11) that the clear-cut V-I characteristic predicted for tunneling sandwiches formed of superconductors with

Figure 5 V-I characteristics for a Sn-Pb sandwich at (bottom to top) 3.75°K, 3.70°K, and 3.60°K, respectively. The voltage scale (vertical) is 0.5 mv per large division and the current scale is 50 µamp per large division for all three characteristics.

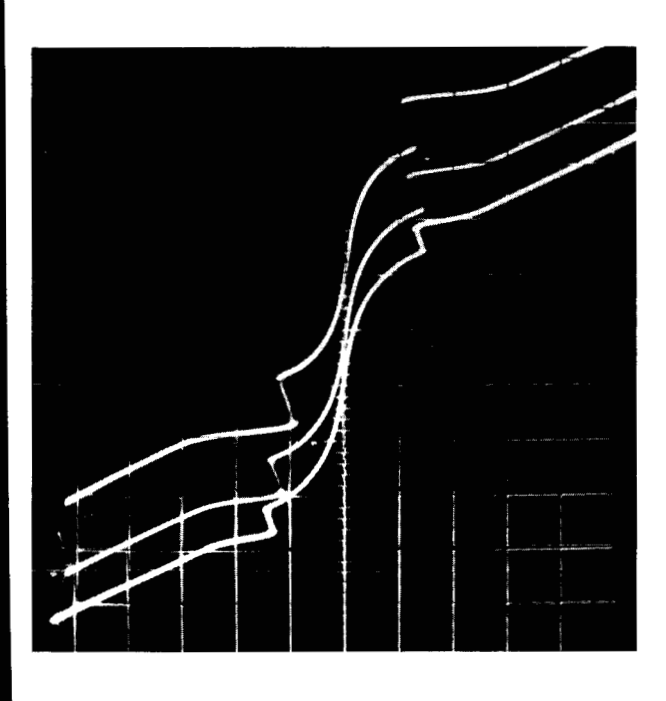
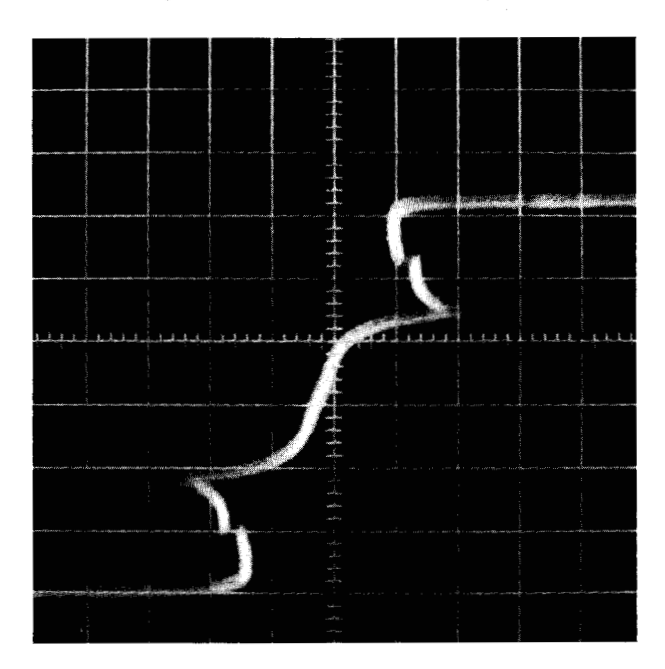


Figure 6 Portion of a V-I characteristic for a Sn-Pb sandwich showing, with an expanded current scale, the predicted cusp at the lower voltage limit of the negative resistance region. The break in the characteristic within the negative resistance region is attributed to the onset of oscillation.



widely different energy gap values is no longer exhibited when the gap values become nearly equal. The calculated curves of Figs. 10 and 11 are broken at the point where a mathematical singularity in the current occurs—namely at the voltage $\varepsilon_{\rm Sn}-\varepsilon_{\rm In}$. Note the change in current scale in Fig. 11. On the current scale of Fig. 10, the current variation below approximately 2 mv at 2.0°K is not visible. Again, at least qualitatively, the calculated curves and experimental results are in agreement. No attempt has been made to follow in detail the changes that occur in the characteristics according to the equations of the Analysis Section as the two energy gaps approach each other in value

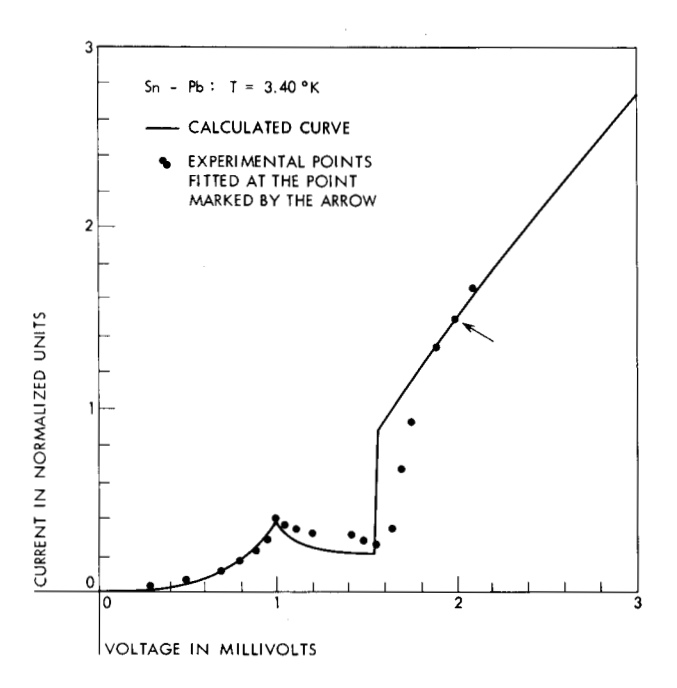
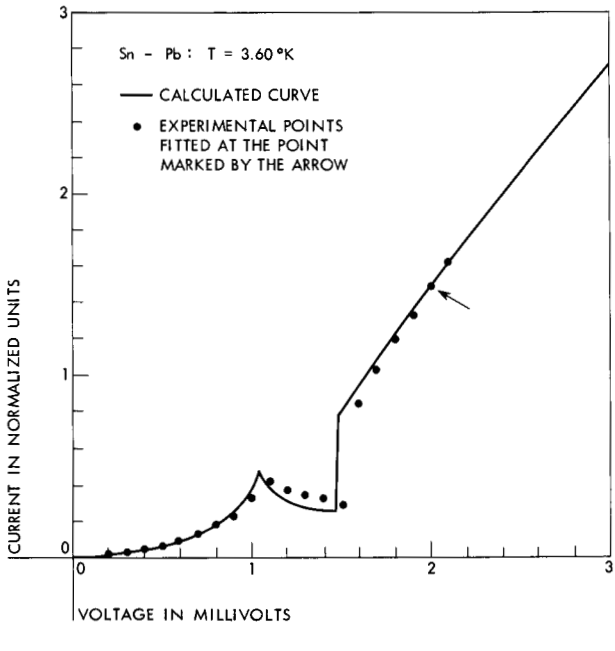


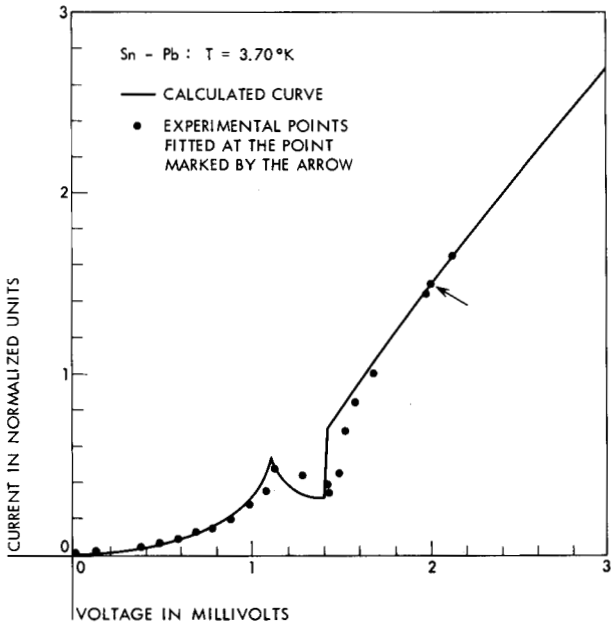
Figure 7 (a) Comparison for a Sn-Pb sandwich at 3.40°K between the calculated I-V characteristic (solid curve) and experimental points taken from photographs such as those of Fig. 5. The current was normalized so that the point marked by the arrow fell on the curve. Experimental values for the energy gaps were used in the calculations.

- (b) Comparison for a Sn-Pb sandwich at 3.60°K.
- (c) Comparison for 3.70°K.

Conclusions

Detailed calculations based on a simple model of electron tunneling are in excellent agreement with experiments involving tunneling through a thin dielectric layer between a normal and a superconducting metal and between two superconducting metals, at least so long as the energy gaps involved are appreciably different from one another. The relative ease of experimentation employing the tunneling technique, coupled with the fact that it provides a direct measure of the energy gap of a superconductor, suggests its applicability to a variety of problems in superconductivity. Among these are the determination of





40

anisotropy in the energy gap for single-crystal specimens, delineation of the variation of the energy gap at the surface of inhomogeneous superconductors, and the elucidation of the possible position dependence of the energy gap, 14 particularly in laminar super-conductors. 15,16

Appendix

In order to show that the singularity in current is logarithmic let $V = \varepsilon_2 - \varepsilon_1 - \eta$ in I_1 , and investigate the behavior of the integral for small values of η . Let

$$I_{1} = \int_{\varepsilon_{2}-V}^{\infty} \frac{E(E+V)}{\sqrt{E^{2} - \varepsilon_{1}^{2}} \sqrt{(E+V)^{2} - \varepsilon_{2}^{2}}}$$

$$\times \phi(-E, V) dE \tag{A1}$$

$$V = \varepsilon_2 - \varepsilon_1 - \eta \tag{A2}$$

$$E = u + \varepsilon_1 + \eta . \tag{A3}$$

Table 1 Full Limiting Value of the Energy Gap ($2\varepsilon_0$)

Super- conductor	Transition Temperature (T_c) for This Work	This Work		Giaever and Megerle ^(a)		Richards and Tinkham ^(b)	Ginsberg and Tinkham ^(c)
		mv	$2\varepsilon_0/kT_c$	mv	$2\varepsilon_0/kT_c^{(d)}$	$2\varepsilon_0/kT_c^{\rm (d)}$	$2\varepsilon_0/kT_c^{(d)}$
Al	1.30°K	0.28 ± 0.03	2.50 ± 0.30	0.32 ± 0.03	3.20 ± 0.30	3.20 ± 0.10 ^(e)	
Sn	3.80°K	1.02 ± 0.02	3.10 ± 0.05	1.11 ± 0.03	3.46 ± 0.10	3.60 ± 0.20	3.30 ± 0.20
Pb	7.2°K	2.50 ± 0.05	4.04 ± 0.10	2.68 ± 0.06	4.33 ± 0.10	4.10 ± 0.20	4.00 ± 0.50
In	3.40°K	<1 mv	≈3	1.05 ± 0.03	3.63 ± 0.10	4.10 ± 0.20	3.90 ± 0.30

I. Giaever and K. Megerle, Phys. Rev. 122, 1101 (1961).
P. L. Richards and M. Tinkham, Phys. Rev. 119, 581 (1960).
D. M. Ginsberg and M. Tinkham, Phys. Rev. 118, 990 (1960).
These authors use the bulk transition temperature.
From M. A. Biondi and M. P. Garfunkel, Phys. Rev. 116, 853 (1959).

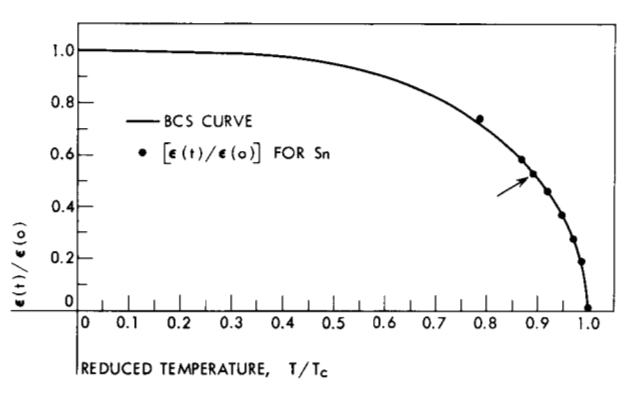
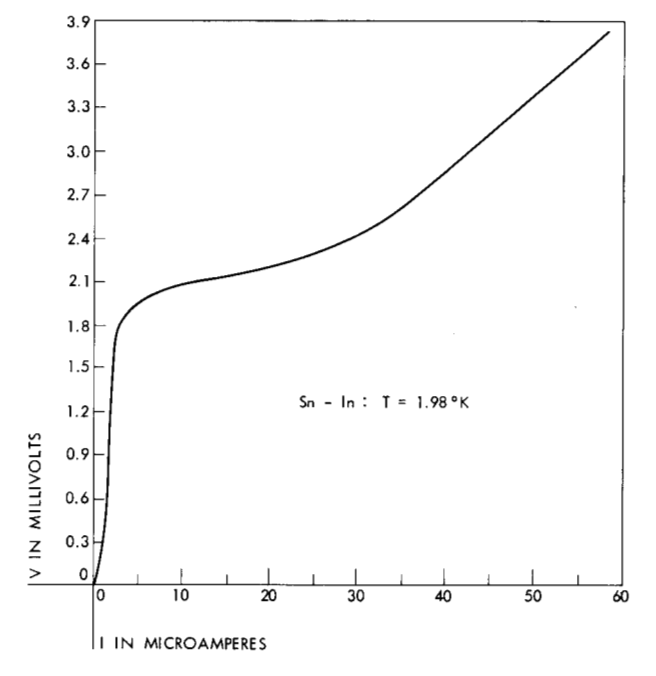


Figure 8 The energy gap for superconducting tin, determined from the V-I characteristics obtained for electron tunneling between superconducting lead and tin, plotted vs reduced temperature and compared with the theoretical curve (solid line) of BCS. The point marked by an arrow was fitted to the curve in order to obtain the limiting full gap value, $2\varepsilon_0 = 3.10kT_c$, with $T_c = 3.80^{\circ}K$.



Voltage vs tunneling current characteristic for a Sn-In sandwich at 1.98°K.

Figure 10 Calculated voltage vs tunneling current characteristic for a Sn-In sandwich at 3.20° K. Note the qualitative similarity to the experimental curve (Fig. 9). The effect of the mathematical singularity in the current, which occurs at the break in the curve at $V = \varepsilon_{\rm Sn} - \varepsilon_{\rm In}$ extends over only a very small voltage interval.

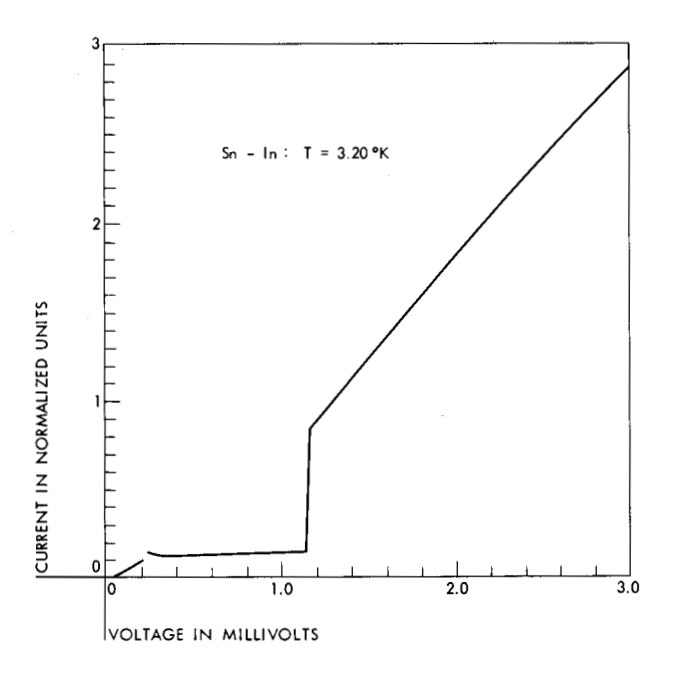
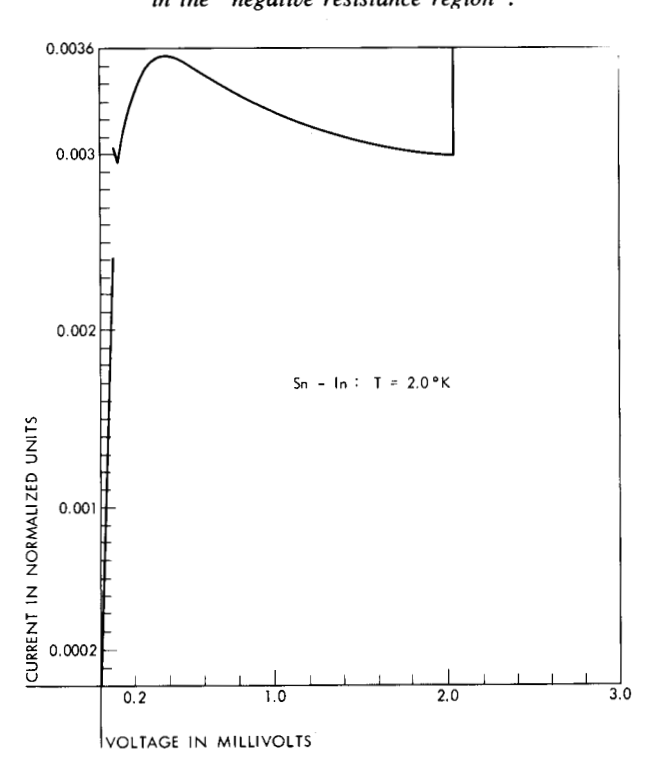


Figure 11 Portion of the calculated voltage vs tunneling current characteristic for a Sn-In sandwich at 2.0°K. The current scale has been expanded in order to show the detail in the "negative resistance region".



Then

$$I_{1} = \int_{0}^{\infty} \frac{(u + \varepsilon_{1} + \eta)(u + \varepsilon_{2})}{\sqrt{u(u + \eta)}\sqrt{(u + 2\varepsilon_{1} + \eta)(u + 2\varepsilon_{2})}}$$

$$\left\{\frac{1}{1 + \exp(-u - \varepsilon_{2})} - \frac{1}{1 + \exp(-u - \varepsilon_{1} - \eta)}\right\} du . (A4)$$

Assume that η may be neglected in comparison with the semigap-widths ε_1 and ε_2 .

$$I_{1} \approx \int_{0}^{\infty} \frac{1}{\sqrt{u(u+\eta)}} \left\{ \frac{(u+\varepsilon_{1})(u+\varepsilon_{2})}{\sqrt{(u+2\varepsilon_{1})(u+2\varepsilon_{2})}} \right.$$

$$\left. \frac{e^{-\varepsilon_{1}} - e^{-\varepsilon_{2}}}{[1+\exp(-u-\varepsilon_{1})][1+\exp(-u-\varepsilon_{2})]} \right\} e^{-u} du \quad (A5)$$

or
$$I_1 \approx \int_0^\infty \frac{g(u)e^{-u}}{\sqrt{u(u+\eta)}} du$$
 (A6)

or
$$I_1 \approx \int_0^1 \frac{g(u)e^{-u}}{\sqrt{u(u+\eta)}} du + \int_1^\infty \frac{g(u)e^{-u}}{\sqrt{u(u+\eta)}} du$$
. (A7)

The second integral on the right is a constant C for small values of η , so it need not be discussed further.

The expression $g(u)e^{-u}$ has upper and lower bounds (say A and B, respectively) which are greater than zero in the interval $0 \le u \le 1$, so

$$A\int_0^1 \frac{du}{\sqrt{u(u+\eta)}} \geqslant I_1 - C \geqslant B\int_0^1 \frac{du}{\sqrt{u(u+\eta)}}.$$
 (A8)

But

$$\int_0^1 \frac{du}{\sqrt{u(u+\eta)}} = \cosh^{-1}\left(\frac{2}{\eta} + 1\right) \approx \ln 4 - \ln \eta , \quad (A9)$$

which exhibits the logarithmic singularity.

Note that the quantity $e^{-\varepsilon_1} - e^{-\varepsilon_2}$ is a factor of the integrand of I_1 in Eq. (A5). Therefore, when $\varepsilon_1 = \varepsilon_2$, the logarithmic singularity does not occur.

Acknowledgments

The authors have benefited from helpful discussions with M. L. Cohen, R. S. Davis, and H. O. McMahon. The assistance of R. M. Sawdo is gratefully acknowledged.

References

- 1. I. Giaever, Phys. Rev. Letters 5, 147, 464 (1960).
- J. Nicol, S. Shapiro, and P. H. Smith, *Phys. Rev. Letters* 5, 461 (1960).
- 3. I. Giaever and K. Megerle, Phys. Rev. 122, 1101 (1961).
- J. Bardeen, L. N. Cooper, and J. R. Schrieffer, Phys. Rev. 108, 1175 (1957).
- 5. J. Bardeen, Phys. Rev. Letters 6, 57 (1961).
- Cf., also, S. Shapiro and P. F. Strong, Bull. Am. Phys. Soc. II, (March, 1961).
- 7. L. C. Hebel, *Phys. Rev.* 116, 79 (1959), contains a discussion of the significance of the rounding-off parameter as well as references to earlier work.
- Such an analysis is very familiar in the treatment of tunneling through semiconductor junctions. Cf., e.g., L. Esaki, Phys. Rev. 109, 603 (1958).

- 9. J. C. Fisher and I. Giaever, J. Appl. Phys. 32, 172 (1961).
- J. L. Miles and H. O. McMahon, J. Appl. Phys. 32, 1176 (1961).
- 11. K. Blodgett and I. Langmuir, Phys. Rev. 51, 946 (1937).
- 12. I. Langmuir, J. Am. Chem. Soc. 39, 1848 (1917).
- 13. Cf., e.g., P. L. Richards and M. Tinkham, *Phys. Rev.* 119, 575 (1960).
- 14. R. H. Parmenter, Phys. Rev. 118, 1173 (1960).
- P. H. Smith, S. Shapiro, J. L. Miles, and J. Nicol, *Phys. Rev. Letters* 6, 686 (1961).
- 16. L. N. Cooper, Phys. Rev. Letters 6, 689 (1961).

Received June 15, 1961